Gait' shear and plantar pressure monitoring: A non-invasive OFS based e-Health solution

Cátia Tavares, M. Fátima Domingues, Anselmo Frizera-Neto, *Member, IEEE,* Tiago Leite, Cátia Leitão, Nélia Alberto, Carlos Marques, Ayman Radwan, *Senior Member, IEEE,* Eduardo Rocon, Paulo André, *Senior Member, IEEE,* Paulo Antunes

***Abstract*—In an era of unprecedented progress in sensing technology and communications, health services are able to evolve towards a close monitoring of patients and elderly citizens, without jeopardizing their daily routines, through health applications on their mobile devices, in what is known as e-Health. Within this field, we propose an optical fiber sensor (OFS) based system for simultaneous monitoring of shear and plantar pressure during gait movement. These parameters are considered to be two key factors in gait analysis which can help in early diagnosis of multiple anomalies, such as diabetic foot ulcerations or in physical rehabilitation scenarios.**

The proposed solution is a biaxial OFS based on two in-line fiber Bragg gratings (FBGs), which were inscribed in the same optical fiber and placed individually in two adjacent cavities, forming a small sensing cell. Such design presents a more compact and resilient solution with higher accuracy, when compared to the existing electronic systems.

The implementation of the proposed elements into an insole is also described, showing the compactness of the sensing cells, which can be easily integrated into a non-invasive mobile e-Health solution for a continuous remote gait analysis of patients and elder citizens. The reported results show that the proposed system outperforms existing solutions, in the sense that it is able to dynamically discriminate shear and plantar pressure during gait.

This work is funded by FCT/MEC through national funds and when applicable co-funded by FEDER – PT2020 partnership agreement under the project UID/EEA/50008/2013.

Cátia Tavares, Nélia Alberto and Ayman Radwan, are with Instituto de Telecomunicações, Campus Universitário de Santiago, 3810-193 Aveiro, Portugal (e-mails: catia.tavares @ua.pt; nelia @av.it.pt, aradwan @av.it.pt).

M. Fátima Domingues is with the Instituto de Telecomunicações, Campus Universitário de Santiago, 3810-193 Aveiro, Portugal; Department of Physics & I3N, University of Aveiro, Campus Universitário de Santiago, 3810-193 Aveiro, Portugal and Centro de Automática y Robótica, CSIC-UPM ctra. Campo Real, 28500 Arganda del Rey, Madrid, Spain (e-mail: fatima.domingues @ua.pt).

Anselmo Frizera Neto is with the Telecommunications Laboratory LABTEL,Electrical Engineering Department, Federal University of Espírito Santo, 29075-910, ES, Brazil (e-mail: frizera @ieee.org).

Tiago Leite, Cátia Leitão, Carlos Marques and Paulo Antunes are with Department of Physics & I3N, University of Aveiro, Campus Universitário de Santiago, 3810-193 Aveiro, and Instituto de Telecomunicações, Campus Universitário de Santiago, 3810-193 Aveiro, Portugal (e-mails: tmpl @ua.pt; catia.leitao @ua.pt; carlos.marques @ua.pt; pantunes @ua.pt).

Eduardo Rocon de Lima is with Centro de Automática y Robótica, CSIC-UPM, ctra. Campo Real, 28500 Arganda del Rey, Madrid, Spain (e-mail: erocon @iai.csic.es).

Paulo André is with Department of Electrical and Computer Engineering and Instituto de Telecomunicações, Instituto Superior Técnico, University of Lisbon, 1049-001 Lisbon, Portugal (e-mail: paulo.andre @lx.it.pt).

***Index Terms*—Gait analysis; e-Health application; physical rehabilitation; shear and plantar pressure sensor; biaxial optical fiber sensor; multiplexed fiber Bragg gratings;**

I. Introduction

Lately, we have witness great progress in electronics and networking, leading to a shift in innovation direction. It could easily be noticed that mobile networks have moved from offering applications mainly for entertainment and human communications (i.e. phone calls, messaging, social networking, etc.) towards more vital applications, such as smart cities, e-Health or intelligent transportation systems, collectively known as Internet of Things (IoT). IoT has been receiving much attention from the research and industry communities, due to the foreseen gains that it can bring in enhancing the life quality of citizens and increasing the safety of our environment and society. One of the very hot fields of IoT is e-Health, which has been on the rise due to the change of the population demographics (increase of population over 65 years old). Between 2000 and 2050, the world's population aged over 60 years is expected to double from about 11% (605 million) up to 22% (2 billion), with the group aged 80 years and over growing most rapidly (predictably will quadruple from approximately 100 million to 395 million people). Many elderly and patient groups experience vary degrees of mobility impairments, which requires a closer monitoring. Assistive devices play a pivotal role in their lives and have a great impact on their ability to live independently and perform basic daily tasks. The assistive products market is set to expand significantly in response to the ageing population and disability trends, with a global market for home medical equipment expected to grow from $27.8 billion in 2015 to nearly $44.3 billion by 2020 [1]. This growing demand for e-Health solutions aims to improve both the quality of healthcare services, as well as the life quality of people, by providing them the autonomy and mobility during their daily activities.

The use of electronic and mobile networking in health services (i.e. e-Health) increases the quality given to patients and helps medical staff in early diagnosis of anomalies, when premature display of patients' irregular health conditions is reported. Non-invasive continuous monitoring of individuals' health conditions, rehabilitation status, or assistance appears as a natural evolution of current healthcare services, providing

patients with continuous remote support when required, while guaranteeing autonomy and free mobility. Basically, e-Health is seen as an approach to help elder generations and patients with chronic illness to live an active life, without comprising their mobility or daily routine. Following this direction and towards improving the quality of life of physically impaired citizens by increasing their mobility, our team has been working in different practical solutions for continuous remote monitoring of patients [2-4].

The monitoring and analysis of shear and plantar pressure involved in gait is crucial for the evaluation of patients under physical rehabilitation process, as well as for the control of rehabilitation exoskeletons, in order to correct abnormal plantar pressures due to the uneven load distribution, resultant from the foot poor sensitivity [5, 6]. Moreover, shear in particular, plays a major role in the diagnosis of foot ulceration of diabetic patients. This health condition can occur when the tissue is compressed under pressure during gait/walk. An early discovery of irregularities in the gait pattern of such individuals at risk is the first step to reduce the occurrence of ulceration and its treatment. Although shear stress has been identified as a pathogenic factor in the development of plantar ulcers, due to lack of validated shear stress sensing devices, only studies related to plantar pressures are widely reported [5]. During the last few decades, some methods have been proposed for the measurement of plantar shear stress [5], nonetheless there is a lack of systems able to accurately monitor, simultaneously, shear and plantar pressure during gait. The work reported in this paper intends to fill such gap, while providing an ambulatory solution, based on the state-of-the-art optical fiber sensing technology driven for e-Health applications.

As a first step, we have developed a non-invasive e-Health solution for continuous remote monitoring of foot plantar pressure during gait (walking). Our previous efforts have concentrated on the pressure distribution, through a strategically placed network of optical fiber sensors (OFSs) [2-4]. In the presented work, we take a step forward by presenting the design and implementation of a fiber Bragg grating (FBG)-based platform, for simultaneous measurement of shear and vertical forces, which can be useful in various applications, in addition to e-Health. The proposed architecture comprises a compact and accurate biaxial OFS based on two in-line FBGs (FBG1 and FBG2), placed individually in two adjacent cavities. For the demodulation of the optical signal registered by the designed optical sensing cell, a system of two equations was used, correlating the sensitivities of both FBGs with the vertical (F_V) and shear (F_S) forces [7]. Moreover, we also present the design and integration of the sensing architecture in an insole for continuous monitoring of F_S and F_V (from which is calculated the plantar pressure), during the gait movement of patients.

The rest of this paper is organized as follows. Section 2 provides a survey of the state-of-the-art technology in monitoring shear and vertical forces, highlighting the advantages of the proposed solution. Section 3 introduces the design of the sensors and the implemented experimental protocols. Section 4 presents the calibration results and the sensing cell performance analysis. Section 5 showcases the implantation of 5 sensing cells in an insole for gait analysis purposes. Section 6 discusses the e-Health architecture. Conclusions are drawn in Section 7.

II. Related Work

Vertical force sensors are nowadays required for a wide number of applications, in diverse areas such as industrial production and structural health monitoring, artificial intelligence, robotic exoskeletons and other health applications [2-4], [8-15]. There are several types of F_V sensors, which are characterized essentially by the transduction mechanisms and technology used for converting forces into electrical signals, such as piezo resistivity and capacitance [10, 13-15]. In addition to these electronic mechanisms, other transduction methods, as OFSs are also frequently used for the measurement of these type of forces [2-4, 16].

Apart from the F_V sensors, devices with additional sensing properties, such as temperature and shear, are highly desired in equipment for e-Health applications. Specifically, sensors capable of measuring F_V and F_S simultaneously are highly required for haptic perception of robotic hands, prosthetic skin and to monitor the stress under the foot to prevent its ulceration [2-4, 17-23].

Several studies have been published, using different technologies, for simultaneous monitoring of F_V and F_S, namely: strain gauge technology [20, 24], piezoelectric materials [21, 25], capacitive sensors [26], micro strip antennas and coils [27], to name a few. In this context, OFSs appear as an alternative technology to sense these variables, with several advantages over the electronic counterparts. Such advantages include their immunity to electromagnetic interference, remote operation and sensing capability, small dimensions, lightweight, and geometrical versatility, making this technology increasingly used as sensing devices in several areas, with special significance in the biomedical engineering and biomechanics areas [2-4, 8, 28, 29].

Although few, there are already some works reporting the development of optical fiber based F_V and F_S sensors. In 2000, Koulaxouzidis *et al.* demonstrated that three optical fibers with one FBG each (one on the horizontal and the other two on the diagonals), embedded in a block of solid elastomer, could be used for the measurement of in-shoe shear stress [30]. The Bragg wavelength shift was found to be almost linear under shear stress, in the range between -120 kPa and 120 kPa, yielding to a sensitivity of 4.35 pm/kPa. In 2013, Zhang *et al.* used a similar method to produce a sensor for the measurement of the same parameters. However, in this case only two optical fibers with FBGs were used (one on the horizontal and the other on the diagonal directions), embedded in a soft polydimethylsiloxane matrix [7]. The sensitivities were found to be 0.82 pm/Pa for vertical pressure and 1.33 pm/Pa for shear. Also, previously, in 2005, Wang *et al.* used a different sensing mechanism, consisting of an array of optical fibers, lying in perpendicular rows and columns

separated by elastomeric pads [31]. In the reported design, the measurements of plantar and shear pressures are based on intensity attenuation in the fibers due to physical deformation. The pressure measurement relies on the force induced light loss from the two affected crossing fibers, while the shear measurement depends on relative position changes in these pressure points between the two fiber mesh layers. This method was later used by other researchers [32-34], where they tried to improve the quality of the obtained data, but still with the disadvantage of the high number of fibers for each measuring point, hence high complexity of the sensor.

Although some previous efforts reported the use of OFSs, all those works have used complex designs, which increase their fragility and lowered their application feasibility.

With the aim of reducing the complexity of the sensing device without compromising its performance, we present the design and implementation of an FBG-based sensor for simultaneous measurement of F_V and F_S.

Our proposed solution stands out from the previously reported ones by the minimalism of the sensor structure, with yet an accurate feedback.

III. Sensing Cell Design and Implementation

A. *Sensing cell design*

In the designed architecture, we used a sensing system comprising two multiplexed FBGs with a 2 mm-length, FBG1 and FBG2, spaced by 9 mm, inscribed in a photosensitive optical fiber (GF1, Thorlabs®), using the phase mask method with an UV KrF pulsed excimer laser (Bragg Star^{TM} Industrial-LN, Coherent) operating at 248 nm. The pulse energy applied was of 5 mJ, with a repetition rate of 500 Hz. The central Bragg wavelength of the FBGs is 1560.9 nm and 1557.6 nm, for FBG1 and FBG2, respectively.

The optical fiber containing the multiplexed FBGs was incorporated in a small cell (9.0 mm x 16.0 mm x 5.5 mm) composed by two cavities, as shown in Fig. 1a). The cavity in which the FBG1 was placed (cavity 1) was mechanically isolated with a cork wall with a thickness of 2 mm, while the cavity containing the FBG2 (cavity 2) was designed and 3D printed with a hard polymer (polylactic acid, PLA) with a 1.2 mm thick wall. To protect the optical fiber and provide the necessary robustness to the sensing cell, both cavities were then filled with an epoxy resin [16]. Despite the epoxy resin stiffness, the applied F_V and F_S still induces deformation in the cell area and consequently, in the optical fiber sensors, without compromising their feedback. It should be noted that no bonding points were added in the cross section between the optical fiber and the cavities boundaries. In that way, a vertical force applied in the cell top area will compress the epoxy resin vertically, inducing the stretching of the fiber embedded in its interior. On the other hand, a horizontal force, applied along the longitudinal axis of the fiber (left to right on the image), will compress the resin, and the fiber containing the sensors against the PLA hard wall.

Due to its near zero Poisson coefficient [35], the cork walls in cavity 1 provide the necessary mechanical isolation from lateral forces (applied out of the sensing cell area), while, simultaneously, offering the necessary elasticity for the FBG1 to be actuated under vertical forces and longitudinal shear stresses.

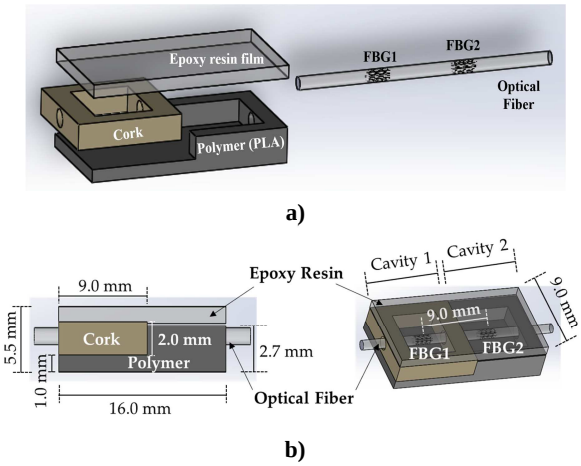

Fig. 1. Schematic illustration of the designed sensing cell for simultaneous F_V and F_S measurement: a) individual components and b) finalized cell structure.

Additionally, in order to induce different sensitivities in the FBGs, the walls of cavity 1 were designed to be slightly higher than the walls from the cavity 2 (gap of 0.8 mm), and in that way, the response obtained from FBG1 can be enhanced when compared with the FBG2, since the latter is more concealed due to the hard polymer wall. To make the contact area uniform, a 2 mm thick layer of epoxy resin was placed on the top of the sensing cell, as shown in Fig. 1b).

B. *Calibration and performance testing methodology*

Since the optical sensing cell feedback is processed in terms of the Bragg wavelength shift ($\Delta\lambda$), for the demodulation of the reflected optical signal, it was necessary to calibrate each FBG, independently, to F_V and F_S. To do so, a 3-axial electronic force sensor, composed by one biaxial (MBA400, Futek) and one uniaxial (Transdutec, TPP-3/75) units, was used. The designed optical fiber based sensing cell (designated hereinafter as FBGs cell) was firmly attached to the three-axial sensing unit, in order to guarantee that any perturbation induced in the FBGs cell would be also registered by the electronic sensing mechanism. Fig. 2 is a schematic representation of the experimental setup implemented. The data retrieved from the electronic sensor was acquired through an analog-to-digital converter (USB-6008, National Instruments), while the optical signal given by the FBGs cell

was acquired by an interrogation system (I-MON 512 USB, Ibsen).

For the calibration of the FBGs cell to F_S, a metal slide, placed between the sensing units and a metal cylinder bar (3 kg), was horizontally dragged with the help of a translation stage [7], as shown in Fig. 2. The translation stage pushed the metal slide parallel to the sensors' top area, inducing a F_S in both sensing units (electronic and optical). During this test, the F_V was maintained constant ($\Delta F_V \approx 0$ N). For the calibration to F_V, a variable force was applied on the cylindrical bar, while the F_S was kept constant ($\Delta F_S \approx 0$ N). During these procedures (F_S and F_V calibration), the values registered by both sensing systems were simultaneously acquired for further comparison/calibration.

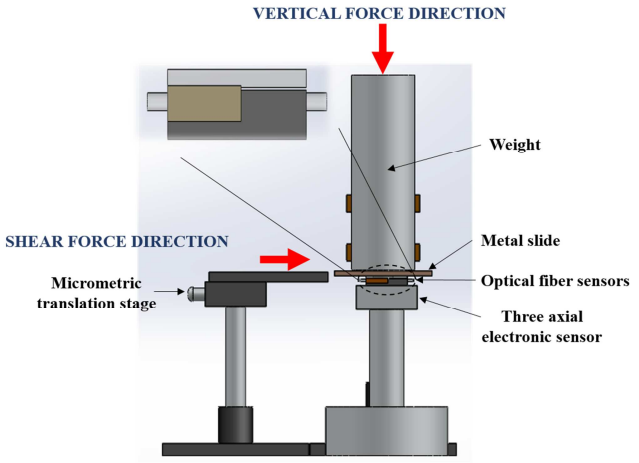

Fig. 2. Representation of the implemented experimental setup for the calibration and testing of the FBGs cell.

After the calibration, in order to evaluate the FBGs performance under simultaneous application of F_V and F_S, the procedures described previously were performed simultaneously: the metal slide was propelled horizontally, while a F_V was applied in the cylindrical bar, as seen in Fig. 2. During the implementation of this protocol, both sensors (electronic and optical) were simultaneously acquiring the data modulated in the sensing units. The obtained results are presented and discussed in the next Section *C* and *D*.

C. Calibration results

Fig. 3 shows the data simultaneously acquired by the electronic and optical systems, for the F_V (a) and F_S (b) characterization procedures. From the F_V characterization, Fig. 3a), it is notorious the increase of the registered pressure with the load applied along the time. In the case of the optical sensor, this increase is translated by a continuous wavelength shift towards higher wavelengths in both FBGs. Such shift is caused by the longitudinal distension (stretching) of the resin under vertical compression, which will induce the elongation of the embedded optical fiber, and therefore the positive wavelength shift.

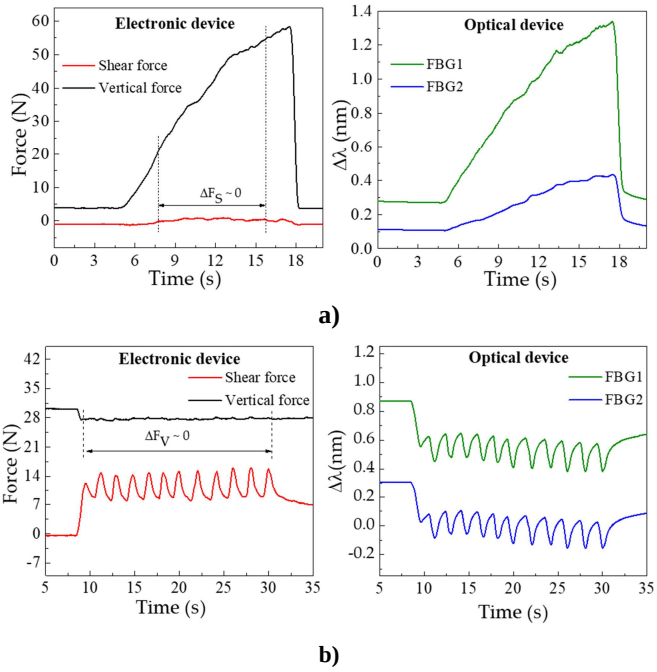

Fig. 3. Data acquired by the three-axial electronic (left) and optical fiber (right) based systems, for the **a)** vertical and **b)** shear forces characterization.

In the representation of the shear calibration data (see Fig. 3b), the periodic variations induced by the translation stage movements are visible in both sensors. In the electronic device, the increasing force corresponds to the movement of the translation stage given by one complete turn of the micrometric screw (360°). Once that turn is complete, there is a relaxing moment till the new turn is started, which corresponds to the decrease (return to initial state) of the applied force. In the represented characterization process, there is a total of 12 turns. In the optical sensor response, this data is inverted, hence the shear applied in the cell will longitudinally compress the resin and the embedded optical fiber, resulting in a negative wavelength shift.

From the characterization procedures, the sensitivities of FBG1 and FBG2 were calculated for both the vertical and shear forces applied. Towards that, for each value registered by the three-axial electronic sensor, the correspondent Bragg wavelength shift (given by the optical sensor) was correlated, as presented in Fig. 4. From the calibration representation, a linear dependence of the Bragg wavelength shift with the applied force is verified. The sensitivities obtained for each FBG as a function of the vertical (K_{1V} and K_{2V}) and shear forces (K_{1S} and K_{2S}) were:

$K_{1V} = (14.15 \pm 0.10) \times 10^{-3}$ nm/N, $K_{1S} = (-26.02 \pm 0.08) \times 10^{-3}$ nm/N,
$K_{2V} = (7.35 \pm 0.02) \times 10^{-3}$ nm/N, $K_{2S} = (-24.29 \pm 0.08) \times 10^{-3}$ nm/N.

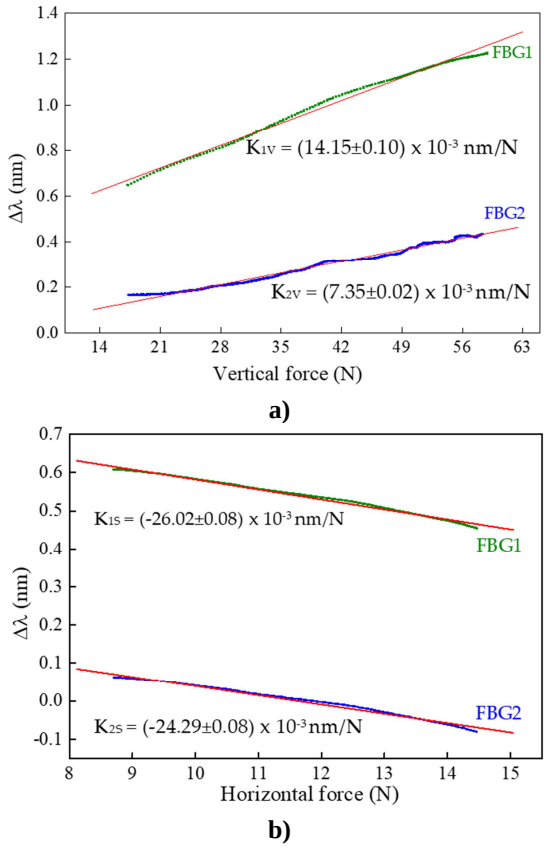

Fig. 4. Calibration data obtained for FBG1 and FBG2 during the variation of the applied forces: **a)** vertical (with $\Delta F_S \approx 0$ **N**) and **b)** shear (with $\Delta F_V \approx 0$ N). Symbols are the acquired data and the red line corresponds to the linear fit ($R^2 > 0.99$).

The substantial discrepancy in the vertical force sensitivity values obtained for the two FBGs is due to the height difference between the walls of cavity 1 and 2, since there is a gap of 0.8 mm between the wall of cavity 2 and the top of the cell. However, once the fiber is not fixed in any point of the cell, its longitudinal movements are similarly transmitted to FBG1 and FBG2, and therefore their sensitivities to shear forces are not as different as to vertical forces.

D. Implementation: Simultaneous F_V and F_S load

After the calibration, and using the same experimental setup as depicted in Fig. 2, the sensor was tested for simultaneous F_S and F_V loadings. The Bragg wavelength shifts, modulated in the optical fiber sensors under simultaneous shear and vertical loadings, can be related to the applied forces by a two-equation system [7]:

$$\begin{bmatrix} F_V \\ F_S \end{bmatrix} = \begin{bmatrix} K_{1V} & K_{1S} \\ K_{2V} & K_{2S} \end{bmatrix}^{-1} \begin{bmatrix} \Delta\lambda_{FBG1} \\ \Delta\lambda_{FBG2} \end{bmatrix} \Leftrightarrow$$

$$\begin{bmatrix} F_V \\ F_S \end{bmatrix} = \begin{bmatrix} 14.15 \times 10^{-3} & -26.02 \times 10^{-3} \\ 7.35 \times 10^{-3} & -24.29 \times 10^{-3} \end{bmatrix}^{-1} \begin{bmatrix} \Delta\lambda_{FBG1} \\ \Delta\lambda_{FBG2} \end{bmatrix} \quad (1)$$

where $\Delta\lambda_{FBG1}$ and $\Delta\lambda_{FBG2}$ are the Bragg wavelength shift of FBG1 and FBG2, respectively.

In Fig. 5 are presented the values acquired for the electronic and optical sensing units during this test, as well as the data resulting from the application of (1). The plot in Fig. 5a) corresponds to the values registered by the 3-axial electronic force sensor, while the data depicted in Fig. 5b) are the corresponding Bragg wavelength shift values acquired through the optical sensing cell.

After applying (1) to the Δλ values obtained from the optical sensing unit, it is possible to obtain the correspondent force values, as presented in Fig. 5c), which match the values acquired by the electronic sensor.

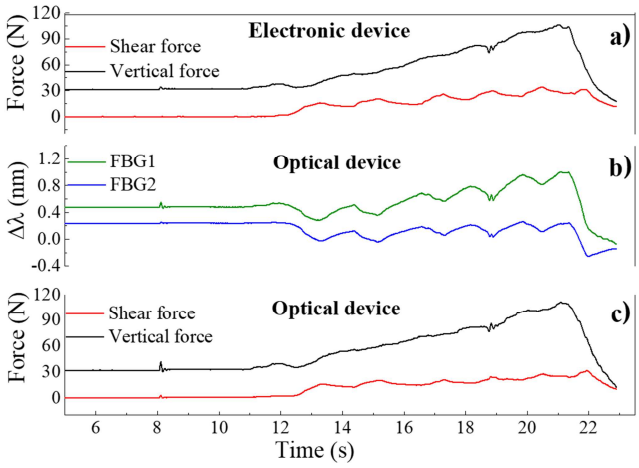

Fig. 5. Response to the applied forces as function of time for: a) the electronic sensor; b) the FBGs cell, with the response as Bragg wavelength shift; c) the FBGs cell, the forces are calculated by applying (1) to the registered wavelength shifts.

Moreover, when comparing both sensors' responses, the differences between the curves obtained by the optical and the electronic sensor have a normalized root mean square error value of $RMSE_V = 0.025$ for F_V and $RMSE_S = 0.053$ for F_S, as presented in Fig. 6, indicating the reliable performance of the optical sensor and its suitability to monitor F_V and F_S, simultaneously.

The compactness, accuracy and reliability of the presented solution will be tested in shoe insoles for non-invasive gait pattern analysis, but its application in rehabilitation exoskeletons robots can also be considered.

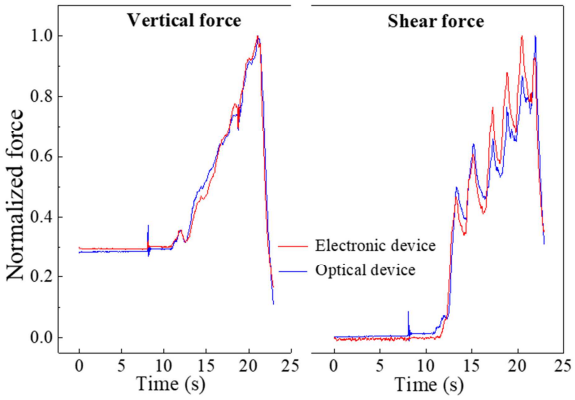

Fig. 6. Comparison between the normalized values acquired with the three-axial sensor and the FBGs cell ($RMSE_V$= 0.025 and $RMSE_S$= 0.053).

IV. Gait Simultaneous Shear and Plantar Pressure Monitoring

In this section we present the integration of the sensing architecture described before in an insole for the continuous and simultaneous monitoring of shear and plantar pressure during gait. This proposed solution is compact in size; non-invasive and could be used continuously during daily routine, without jeopardizing the mobility of patients nor their autonomy, while providing an early assessment of the gait pattern abnormalities of individuals at risk.

A. Insole design and implementation

Considering the foot plantar anatomy, the most at risk areas to develop neuropathic ulcers are the regions covering the bony prominences, where the load is heavily applied. Such areas are located under the metatarsal heads, nonetheless, also the shear stress measured in the great toe and heel are often reported as key points of analysis [5].

Bearing in mind such areas, we have designed and produced an insole incorporating a total of 5 sensing cells, similar to the one described in Section III. A single optical fiber, containing a total of 10 FBGs was incorporated in the insole, as depicted in Fig. 7.

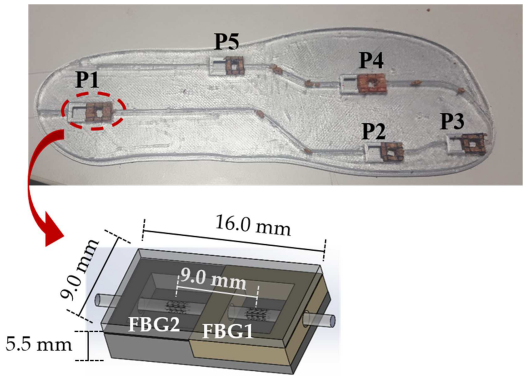

Fig. 7. Photograph of the insole used for shear and plantar pressure monitor, incorporating five FBGs cells (as also schemed).

The FBGs cells were placed in the key points of analysis for the foot plantar pressure and shear stress monitor, namely, heel (P1), midfoot (P5), metatarsal (P2 and P4) and toe (P3).

B. Shear and plantar pressure results

With the developed system, by monitoring the wavelength shift registered by the FBGs in each cell, it is possible to simultaneously monitor the patient's gait pattern, as well as the plantar pressure (corresponding to the vertical force mention in previous sections, for unit of area) and shear stress distribution. Nonetheless, prior to its dynamic application, it is necessary to calibrate each sensing cell to pressure and shear. In that way, the procedure described in Section III *B* was performed individually for each sensing cell, from which the sensitivities values K_{1V}, K_{2V} (to vertical forces) and K_{1S}, K_{2S} (to shear) were obtained for each FBGs cell.

Fig. 8 displays the optical spectra obtained for the developed insole, during the vertical force calibration of the FBGs cell "P5". Since the whole system is placed in one optical fiber with 10 multiplexed FBGs, the Bragg wavelength corresponding to each FBG is also visible. However, during the calibration process, only the FBGs corresponding to the sensing cell inserted in P5 responds to the local applied loads. Such characteristic confirms the good isolation of the designed sensing cell to forces applied in its surroundings, and its suitability for a precise local analysis. Additionally, the presented design (size, number and location of the sensing cells), can be customized according to a doctor prescription and each patient/situation specific needs.

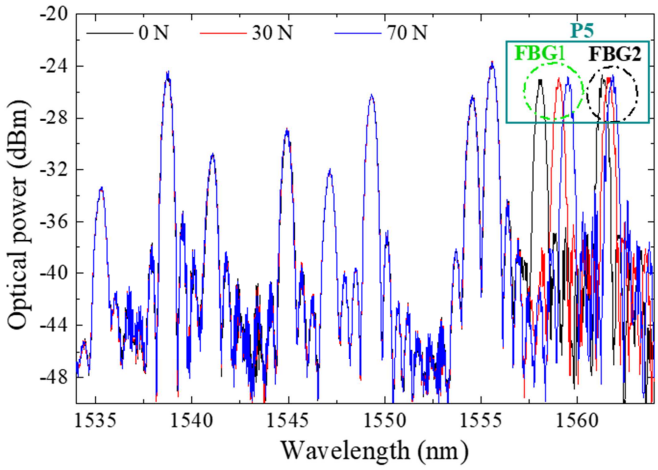

Fig. 8. Optical spectra obtained during the pressure calibration of FBGs cell "P5".

After calibration, the insole was placed in a shoe for a dynamic monitoring test. During such test, the interrogation system was continuously acquiring the Bragg wavelength shift registered in each point, while the subject (female with 45 kg) was walking. Fig. 9 represents the registered wavelength shift for each FBG, in the 5 points, during a 3 seconds gait. Due to a malfunction in the interrogation system, the Bragg wavelength acquired for FBG1 in P1 had extensive value gaps

along time (Bragg wavelength returned as zero) and therefore its values were ignored.

For the global set of the remaining sensing cells, it is clear that each point is activated according to the pressure pattern expected during gait. The stance phase (foot in contact with the floor) and swing phase (foot without contact with the floor, represented with grey shade) are also clear in this representation [2].

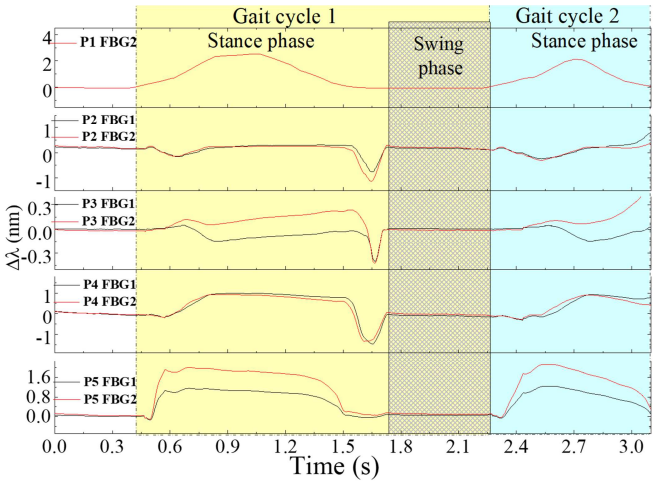

Fig. 9. Wavelength shift in time, registered for each FBG in the 5 points of analysis.

In order to retrieve the values of plantar vertical and shear forces from the raw data plotted in Fig. 9, we apply (1) to each point. The resultant curve, obtained for point 2, located at one of the metatarsal heads (critical point for shear analysis), is depicted in Fig. 10.

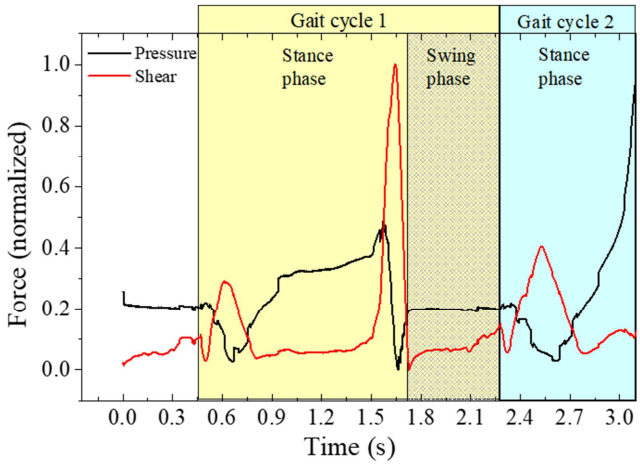

Fig. 10. Plantar pressure and shear stress retrieved from the sensing cells in the insole during gait.

As it can be seen, it is possible to differentiate the plantar vertical force and the anterior-posterior (AP) shear stress curve, as reported previously [2, 5]. From the obtained curves, it is also observed that the maximum shear stress occurs first in the beginning of the foot-flat phase and again, with higher intensity, at the rising of the heel and the toe-off phase, which corresponds to the backward acceleration force under the metatarsal areas [5].

It should also be noted that the shear stress evaluated with the referred system is the AP longitudinal shear, and to evaluate the medial–lateral stress, a different sensing cell configuration should be designed. However, and as stated before (and shown in Fig. 8), lateral forces do not affect the proposed sensing cells performances for AP shear stress and plantar pressure.

Therefore, the designed system presented in this paper is a reliable solution for simultaneous monitoring of plantar pressure and shear stress during gait. Its application as e-Health tool can provide a clear advantage to patients prone to develop neuropathic ulcers, by early alerting them to correct their posture and walking pattern. Also, the incorporation of such devices in rehabilitation exoskeletons will allow the mitigation of the existing gap regarding the monitoring of shear forces.

V. Overall e-Health Architecture

It has been emphasized throughout this paper the importance of the compact size of the sensing architecture, in addition to its resilience. These two properties render the architecture suitable for integration within a non-invasive e-Health system for continuous monitoring of patients and elder citizens. The proposed insole design, described in Section IV, comprises one part of the whole mobile e-Health solution, used to continuously monitor patients for irregularities in their gait movement. The overall non-invasive monitoring solution is shown in Fig. 11. The system comprises three components: the sensing element, the interrogator system, and the mobile app on a smartphone.

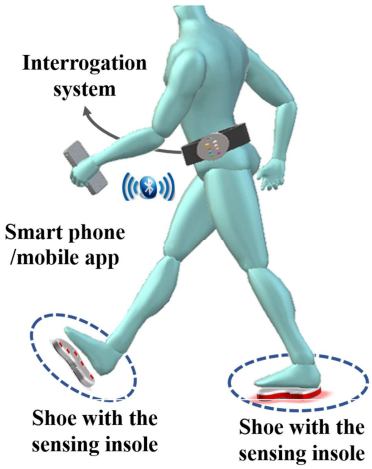

Fig. 11. Non-invasive e-Health optical fiber sensing architecture for shear and plantar pressure gait analysis.

The first part, which is the optical fiber sensing architecture, has been extensively explained throughout the paper. It is basically represented by the insole integrated with the optical FBGs cells, as explained in previous section.

The second part is the interrogator system, required to acquire the signal modulated in the sensing points. This can be translated into shear and vertical pressure, based on the proposed system of two equations, as explained in Section III.

The third and last component is a mobile app installed on a smartphone. The mobile app has multiple roles. First, it is used as a data processing tool to analyze the acquired measurements from the sensing system. Second, the app uses the smartphone as a gateway for transmitting the measured data to the cloud. Additionally, the app can be used to display the results, when required by the patient. The user (patient or his/her doctor) is able to use the app to view instantaneous results or statistics from the measured data over a period of time. The results are continuously transmitted to the cloud for more elaborated analysis by the medical personnel (i.e. the doctor, nurse or physical therapist).

VI. Conclusion

In this work, a novel compact and efficient optical fiber based solution for simultaneous sensing of vertical and shear forces is presented. The proposed architecture is accurate and resilient compared to existing solutions. The results obtained from developed sensing cell show similar behavior to the three-axial electronic force sensor used for comparison, with a $RMSE_V = 0.025$ and $RMSE_S = 0.053$ between them. These values show that the developed device achieved the necessary accuracy, while offering all optical fiber sensors technology advantages, like immunity to electromagnetic interference and humid environments. Moreover, the proposed one-dimensional configuration is a reliable solution, which facilitates the production and incorporation of the sensing cell elements in other devices. Additionally, the presented sensing element, being able to infer and discriminate shear from vertical forces, has a great potential for incorporation into insoles for the measurement of plantar pressure (vertical force) and shear force. This is relevant information in different contexts/scenarios, including the prevention and study of pressure ulcers or in monitoring the performance of athletes during training; in electronic skin (e-skin) technologies; intelligent and rehabilitation robotic exoskeletons; human-machine interaction devices or even biomimetic prosthesis. A complete non-invasive e-Health solution, based on the proposed sensing element, is also presented, which shows its advantages in the continuous monitoring of patients and elder citizens during their active lifestyle routines, without jeopardizing their mobility or freedom.

Acknowledgments: This work is funded by FCT/MEC through national funds and when applicable co-funded by FEDER – PT2020 partnership agreement under the projects UID/EEA/50008/2013, and IT internal project WeHope. Cátia Tavares acknowledges the financial support from WeHope project (ref. 818/2016). The authors acknowledge the financial support from FCT through the fellowships SFRH/BPD/101372/2014 (M. Fátima Domingues), SFRH/BPD/109458/2015 (Carlos Marques) and researcher grant ref. IF/01393/2015 (Ayman Radwan). Nélia Alberto acknowledges the financial support from the PREDICT project (FCT, IT-LA). Anselmo Frizera-Neto acknowledges CAPES PGPTA (88887.095626/2015-01), CNPq (304192/2016-3) and FAPES (72982608, 80599230). Eduardo Rocon acknowledges the financial support from the XoSoft project, Soft modular biomimeticexoskeleton to assist people with mobility impairments, contract H2020–ICT24–2016–688175.

References

[1]- A. McWilliams, “Global markets and technologies for home medical equipment”, bccResearch, Jan. 2016.

[2]- F. Domingues, C. Tavares, C. Leitão, A. Frizera-Neto, N. Alberto, C. Marques, A. Radwan, J. Rodriguez, O. Postolache, E. Rocon, P. André, P. Antunes, “Insole optical fiber Bragg grating sensors network for dynamic vertical force monitoring,” *J. Biomed. Opt.*, vol. 22, no. 9, pp. 091507-1–091507-8, 2017.

[3]- F. Domingues, N. Alberto, C. Leitão, C. Tavares, E. Rocon, A. Radwan, V. Sucasas, J. Rodriguez, P. André, P. Antunes, “Insole optical fiber sensor architecture for remote gait analysis-an eHealth Solution,” *IEEE Internet Things J.*, 2017, doi: 10.1109/JIOT.2017.2723263.

[4]- M.F. Domingues, C. Tavares, N. Alberto, C. Leitão, P. Antunes, P. André, E. Rocon, V. Sucasas, A. Radwan, J. Rodriguez. (2017, Dec.). Non-invasive insole optical fiber sensor architecture for monitoring foot anomalies. Presented at GLOBECOM 2017 - 2017 IEEE Global Communications Conference.

[5]- S. (née Kärki) Rajala, J. Lekkala, “Plantar shear stress measurements - A review,” *Clin Biomech*, vol. 29, no. 5, pp. 475-483, 2014.

[6]- C. Bayón, S. Lerma, O. Ramírez, JI. Serrano, MD. Del Castillo, R. Raya, JM. Belda-Lois, I. Martínez, E. Rocon, “Locomotor training through a novel robotic platform for gait rehabilitation in pediatric population,” *J Neuroeng Rehabil*, vol. 13, no. 98, 6pp, Nov. 2016.

[7]- I. Mohammad, H. Huang, “Pressure and shear sensing based on microstrip antennas,” Proc. SPIE, Sensors and Smart Structures Technologies for Civil, Mechanical, and Aerospace Systems 2012, vol. 8345, 2012.

[8]- C. Leitão, P. Antunes, J.L. Pinto, J. Bastos, P. André, “Carotid distension waves acquired with a fiber sensor as an alternative to tonometry for central arterial systolic pressure assessment in young subjects,” *Measurement*, vol. 95, pp. 45–49, 2017.

[9]- M. Hammock, A. Chortos, B. Tee, J. Tok, Z. Bao, “25th Anniversary article: The evolution of electronic skin (E-Skin): A brief history, design considerations, and recent progress,” *Adv. Mater.*, vol. 25, no. 42, pp. 5997–6038, Nov. 2013.

[10]- N. Luo, W. Dai, C. Li, Z. Zhou, L. Lu, C. Poon, S.-C. Chen, Y. Zhang, N. Zhao, “Flexible piezoresistive sensor patch enabling ultralow power cuffless blood pressure measurement,” *Adv. Funct. Mater.*, vol. 26, no. 8, pp. 1178–1187, Fev. 2016.

[11]- S. Jung, J. Kim, J. Kim, S. Choi, J. Lee, I. Park, T. Hyeon, D. Kim, “Reverse-micelle-induced porous pressure-sensitive rubber for

wearable human-machine interfaces," *Adv. Mater.,* vol. 26, no. 28, pp. 4825–4830, July 2014.

[12]- E. Mesquita, A. Arêde, R. Silva, P. Rocha, A. Gomes, N. Pinto, P. Antunes, H. Varum, "Structural health monitoring of the retrofitting process, characterization and reliability analysis of a masonry heritage construction," *Journal of Civil Structural Health Monitoring*, vol. *7*, no. 3, pp. 405–428, July 2017.

[13]- K. Minami, Y. Kokubo, I. Maeda, S. Hibino, "Analysis of actual pressure point using the power flexible capacitive sensor during chest compression," *J. Anesth*., vol. 31, no. 1, pp. 152–155, Oct. 2016.

[14]- J. Voinea, S. Butnariu, G. Mogan, "Measurement and geometric modelling of human spine posture for medical rehabilitation purposes using a wearable monitoring system based on inertial sensors," *Sensors*, vol. 17, no. 3, 19pp, Jan. 2017.

[15]- S. Choi, H. Cho, C. Lissenden, "Selection of shear horizontal wave transducers for robotic nondestructive inspection in harsh environments," *Sensors*, vol. 17, no. 5, 15pp, 2017.

[16]- L. Ferreira, P. Antunes, F. Domingues, P. Silva, P. André, "Monitoring of sea bed level changes in nearshore regions using fiber optic sensors," *Measurement*, vol. 45, no. 6, pp. 1527–1533, July 2012.

[17]- Y. Zang, F. Zhang, C. Di, D. Zhu, "Advances of flexible pressure sensors toward artificial intelligence and health care applications," *Mater. Horiz.*, vol. 2, no. 2, pp. 140–156, 2015.

[18]- M. Tiwana, A. Shashank, S. Redmond, N. Lovell, "Characterization of a capacitive tactile shear sensor for application in robotic and upper limb prostheses," *Sens Actuators A Phys*., vol. 165, no. 2, pp. 164–172, Sep. 2010.

[19]- P. Puangmali, K. Althoefer, L. Seneviratne, D. Murphy, P. Dasgupta, "State-of-the-art in force and tactile sensing for minimally invasive surgery," *IEEE Sensors J*., vol. 8, pp. 371–381, 2008.

[20]- W. Chen, P. Lee, S. Park, S. Lee, V. Shim, T. Lee, "A novel gait platform to measure isolated plantar metatarsal forces during walking," *J. Biomech*., vol. 43, pp. 2017–2021, 2010.

[21]- S. Kärki, J. Lekkala, H. Kuokkanen, J. Halttunen, "Development of a piezoelectric polymer film sensor for plantar normal and shear stress measurements," *Sens Actuators A Phys*, vol. 154, pp. 57–64, 2009.

[22]- M. Hamatani, T. Mori, M. Oe, H. Noguchi, K. Takehara, A. Amemiya, Y. Ohashi, K. Ueki, T. Kadowaki, H. Sanada, "Factors associated with callus in patients with diabetes, focused on plantar shear stress during gait," *J. of Diabetes Science and Technology*, vol. 10, no. 6, pp. 1–7, 2016.

[23]- S. Rajala, J. Lekkala, "Plantar shear stress measurements—A review," *Clin. Biomech*., vol. 29, pp. 475–483, 2014.

[24]- M. Yavuz, A. Erdemir, G. Botek, G. Hirschman, L. Bardsley, B. Davis, "Peak plantar pressure and shear locations — relevance to diabetic patients," *Diabetes Care*, vol. 30, pp. 2643–2645, 2007.

[25]- M. Razian, M. Pepper, "Design, development, and characteristics of an in-shoe triaxial pressure measurement transducer utilizing a single element of piezoelectric copolymer film," *IEEE Trans Neural Syst Rehabil Eng*, vol. 11, pp. 288–293, 2003.

[26]- E. Heywood, D. Jeutter, G. Harris, "Tri-axial plantar pressure sensor: design, calibration and characterization," *Conf Proc IEEE Eng Med Biol Soc*, vol. 3, no. 2010-3, 2004.

[27]- N. Alberto, L. Bilro, P. Antunes, C. Leitão, H. Lima, P. André, R. Nogueira, J. Pinto, "Optical fiber technology for e-Healthcare," in *Handbook of research on ICTs and management systems for improving efficiency in Healthcare and Social care*. M. Cruz-Cunha, I. Miranda, P. Gonçalves, Hershey PA: IGI Global, pp. 180–200, 2013.

[28]- F. Domingues, A. Radwan, "Optical Fiber Sensors in IoT", in *Optical Fiber Sensors for loT and Smart Devices*. F. Domingues, A. Radwan Springer International Publishing, pp. 73–86, 2017.

[29]- A. Koulaxouzidis, M. Holmes, C. Roberts, V. Handerek, "A shear and vertical stress sensor for physiological measurements using fibre Bragg gratings," *Proceedings of the 22nd Annual International Conference of the IEEE Engineering in Medicine and Biology Society*, vol. 1, pp. 55–58, 2000.

[30]- Z. Zhang, X. Tao, "Soft fiber optic sensors for precision measurement of shear stress and pressure," *IEEE Sensors J*, vol. 13, pp. 1478–1482, 2013.

[31]- W. Wang, W. Ledoux, B. Sangeorzan, P. Reinhall, "A shear and plantar pressure sensor based on fibre-optic bend loss," *J. Rehabil. Res. Dev.*, vol. 42, pp. 315–326, 2005.

[32]- C. Liu, G. Chou, X. Liang, P. Reinhall, W. Wang, "Design of a multi-layered optical bend loss sensor for pressure and shear sensing," *Health Monitoring of Structural and Biological Systems 2007*, Proc. SPIE 6532, no. 65321P, 2007.

[33]- W. Soetanto, N. Nguyen, W. Wang, "Fiber optic plantar pressure/shear sensor," *Health Monitoring of Structural and Biological Systems 2011*, Proc. SPIE 7984, no. 79840Z, 2011.

[34]- C. Chang, C. Liu, W. Soetanto, W. Wang, "A platform-based foot pressure/shear sensor," *Health Monitoring of Structural and Biological Systems 2012*, Proc. SPIE 8348, no. 83481U, 2012.

[35]- S. Silva, M. Sabino, E. Fernandes, V. Correlo, L. Boesel, R. Reis, "R. Cork: properties, capabilities and applications," *Int. Mater. Rev.*, vol. 50, no. 6, pp. 345–365, 2005.